DOI: https://doi.org/10.57233/ihcfs.026

ISBN: 978-978-68-07775

BOOK OF PROCEEDINGS

IHCFS – 2025 WEBSITE: fos.fugusau.edu.ng

1ST INTERNATIONAL HYBRID CONFERENCE OF FACULTY OF SCIENCE

(A PUBLICATION OF FACULTY OF SCIENCE, FEDERAL UNIVERSITY GUSAU, NIGERIA)

SORET IMPACT ON A CHEMICALLY REACTIVE FLUID ALONG A MICROCHANNEL WITH WALL CONCENTRATION FILLED WITH POROUS MATERIALS.

Godwin Ojemeri[1*] and Emmanuel Omokhuale[2]

[1]Department of Mathematics, College of Science, Federal University of Agriculture, Zuru, P. M. B. 28, Kebbi State, Nigeria.

[2]Department of Mathematics, Faculty of Sciences, Federal University Gusau, P. M. B. 1001, Zamfara State.

***Corresponding Author's email:** godwinojemeri@gmail.com

ABSTRACT:

In many industrial processes, a porous medium is used to store, transfer, and distribute energy. Given the porous medium's high surface-to-volume ratio, these topologies deliver thermal performance that is significantly faster than that of conventional energy transmission systems. Thus, the current research investigates the effect of Soret wall-concentration features on a chemically reactive fluid in a superhydrophobic microchannel containing porous materials. One of the parallel plates has been deliberately constructed with a surface that is extremely hydrophobic, while the other has a non-slip surface. We employ a semi-analytical technique (regular perturbation) to address the highly nonlinear ordinary differential equations governing mass diffusion, temperature, and momentum. Illustrative plots were created to show the behavior of major parameters contained in the flow settings. The results of this study show that rising Darcy parameter increases the hydromagnetic flow in the microchannel, resulting in a higher shear stress at the channel walls. Additionally, increasing the thermo-diffusion value optimizes flow behavior. Porous media and the Soret effect have numerous industrial and engineering applications, including the management of geosystems, hydrocarbon storage vessels, phase change processes, isotope splitting, and chemical synthesis.

Keywords: Darcy porous medium, Thermal diffusion, Exothermic fluid, wall concentration, superhydrophobic surface, Microchannel.

INTRODUCTION

When mass and heat are transferred concurrently in a dynamic fluid, the interaction between controlling possibilities and fluxes gets more complicated. It has been found that thermal fluxes may be created not just via thermal simulation but also by concentric forecasting. The thermal-diffusive (Soret) effect describes the mass transfer that occurs as a result of thermal dispersion. These consequences are significant for hydrology, oil reservoirs, nuclear disposal, petrology, nuclear reactors, gas mixes, groundwater pollution migration, geothermal energy, and isotope separation (Kattimani *et al.* 2025). To this goal, Ojemeri *et al.* (2023) investigated the steady-state solutions of a buoyancy-induced chemical reactive fluid in the presence of Soret and radial magnetic field effects in an annular concentric cylinder subjected to suction and injection. Chamuah and Ahmed (2021) described the hydromagnetic free convective dissipative flow over a porous surface in a porous medium influenced by radiation and Soret effects. Ahmed and Bordoloi (2012) investigated three-dimensional flow through a porous vertical plate in a porous medium with sinusoidal suction and permeability influenced by heat diffusion. Bordoloi *et al.* (2023) proposed an analytical solution for two-dimensional steady, viscous, magnetized natural flow over an upstanding porous plate that is evenly extending and immersed in a permeable medium when the thermo-diffusion and chemical reaction impacts are present. Bafakeeh *et al.* (2022) investigated the chemically and thermally

driven time-dependent oscillatory convective flow of a viscous fluid affected by porosity, Hall current, and thermo-diffusion impact. Baoku and Fadare (2018) analyzed the Soret and Dufour consequences for magnetized combined convection in a third-grade fluid across an elastic surface in a Darcy-Forchheimer permeable medium. They concluded that the Soret and Dufour numbers increase with flow and thermal boundary thickness. Usman and Sanusi (2023) investigated the impact of nanofluid flows along a semi-infinite flat plate embedded in a porous medium with heat radiation, Soret, and pressure terms. Because different kinds of nanoparticles are present, they considered the surface temperature and concentration, which fluctuate. Ahmed *et al.* (2024) described how a constant two-dimensional MHD convection-free heat and mass transfer flow via a semi-infinite vertical porous plate is affected by a chemical reaction, magnetic field, thermal radiation, heat sink, and thermal diffusion. The dynamical behavior of Dufor and Soret effects on a Maxwell nanofluid close to a moving sheet, especially when thermophoresis and Brownian motion are present, was clarified by Babu *et al.* (2024).

The study of fluid flow in microchannels with superhydrophobic (SHO) properties and jump temperature is a unique area of increasing interest in heat transfer phenomena with the MHD effect. High repellent qualities, self-cleaning functions, minimized drag forces, and enhanced flow are some advantages of microchannels with SHS. SHS-equipped microchannels can promote self-cleaning behavior and decrease the impact of water exposure on surfaces. Applications for microchannels with SHS include the creation of lab-on-a-chip medical diagnostic devices, controlled microfluidic transport, the separation of water and oil in microfluidic systems, and the improvement of heat transfer by enabling effective liquid flow. (Lee *et al.* 2021). In light of these findings, Ojemeri et al. (2025) investigated the impact of thermal radiation on a buoyancy-induced magnetized Couette flow in an SHO microchannel with Newtonian heating. Hamza *et al.* (2025) studied the effects of dusty fluid in unstable fractional derivatives in Caputo-Fanrizio (CF) and Atangana-Baleanu in Caputo sense (ABC) while solving the heat transfer problem using a SHO microchannel. Furthermore, Hamza et al. (2024a, 2024b) examined the temperature jump scenario and the impact of electrokinetics on natural and combined convection flows in SHO microchannels. Their computational analysis indicates that the SHS and electrokinetic processes contribute to the increased fluid velocity in the microchannel. Magnetized combined flow with permeable medium in an up-facing channel is important in the field of MHD, according to Ojemeri and Onwubuya (2023a). Jha and Gwandu (2018) and (2020) examined fluid flow in an upstanding slit microchannel that had a temperature increase, a magnetic field, and porous material. Sharma et al. (2020) mathematically demonstrate the pressure-induced flow over a microchannel coated with SHS. They found out that, the SHS and electroosmotic effects work to escalate fluid motion in the microchannel. Ojemeri and Onwubuya (2023a) underscored the significance of combined hydromagnetic flow along a porous medium in a SHO microchannel. Other interesting research with varying thermal boundary conditions in the presence of SHS can be seen in the following works: Sia *et al.* (2023), Heidarian *et al.* (2020), and Zhang *et al.* (2019).

Chemical reactive heat transmission (exothermic chemical reaction) via SHO-coated microchannels and slit microchannels has recently aroused researchers' interest due to their prospective uses in engineering and chemical industries, improvements in heat transfer, and applications in biomedical equipment, among others. Microchannels with SHS are finding uses in the creation of lab-on-a-chip medical examination equipment, heat transfer optimization

DOI: https://doi.org/10.57233/ihcfs.026

ISBN: 978-978-68-07775

through streamlined liquid flow, guided microfluidic transport, and oil and water separation in microfluidic systems. To this goal, Ojemeri *et al.* (2024) recently employed a regular perturbation strategy to highlight the influence of heat sink/source fluid on exothermic chemical reaction with heat flow in an SHO-heated microchannel. Ojemeri and Onwubuya (2023b) examined the combined convection flow in a SHO microchannel induced by the interaction of a porous material and a chemically induced heat-absorbing/generating fluid. Later, Ojemeri and Onwubuya (2023c) employed a semi-analytic approach to study the implications of hydromagnetic fluid controlled by Arrhenius kinetics in a microchannel with SHO characteristics and temperature jump circumstances. Hamza et al. (2023b, 2023c) used the homotopy perturbation technique to analyze the effect of a chemically reactive fluid with Hall current on the MHD flow toward a vertical microchannel. Their findings indicate that the growing presence of the Frank-Kamenetskii parameter, which corresponds to the viscous heating term, enhances both thermal and hydromagnetic fluids. Ojemeri *et al.* (2023b) investigated the analytical problem of Arrhenius-controlled fluid in an up-facing microchannel filled with porous medium using the homotopy perturbation technique (HPM) under appropriate boundary conditions. Their findings revealed that differences in the chemical reaction, Darcy number, rarefaction, and wall-ambient temperature factors significantly influence fluid flow and volume flow rate, respectively. Ojemeri and Hamza (2022) proposed a computer model of an Arrhenius kinetically driven heat-generating/absorbing. Their findings suggest that the Frank-Kamenetskii mounting level, which represents the viscous heating term, promotes both thermal and hydromagnetic fluids.

Some chemical engineering procedures, such as polymer manufacture, ceramic or glassware fabrication, and food processing, become more accurate when heat and mass transport occur concurrently in a unique physical shape, such as a slit microstructure. Furthermore, the combined effects of heat and mass with symmetric wall concentration across microchannels with superhydrophobic characteristics on fluid flow have not been fully investigated. Thus, motivated by the knowledge gap identified in the literature review, the goal of this work is to build on Omokhuale and Ojemeri's (2025) work by incorporating and investigating new relationships between heat and mass transfer of an exothermic fluid, the Soret effect, and superhydrophobicity in a microchannel. The simulated nonlinear equations are handled using the regular perturbation approach. The findings of this research will not only help to improve fluid flow in microchannels but will also act as a roadmap for the development of enhanced heat and mass transfer systems for microfluidic equipment and high-performance applications. Furthermore, this unique model can aid in the design of filtration systems and in understanding mass and heat transfer in packed-column reactors and other porous materials used in industrial processes like oil and gas extraction calculations, hydrogeological processes, and so on. More broadly, this model will serve as a basis for understanding and predicting fluid movement in various natural and engineered systems.

MATERIALS AND METHODS

Mathematical Formulation

Imagine a steady, laminar electrically conducting fluid flowing between two upward parallel surfaces with Arrhenius kinetics and equal wall concentration settings. As seen in Figure 1, the wall at $y_0 = 0$ is caused by the exceedingly difficult-to-wet SHO effect, whereas the NSS remains at $y_0 = L$. An applied magnetic field of strength B_0 is stated to be introduced between two upright

DOI: https://doi.org/10.57233/ihcfs.026

ISBN: 978-978-68-07775

microchannel plates. All fluid parameters are considered to be constant. The following assumptions are made in relation to the current formulation:

i. The fluid is steady, incompressible, and obeys Boussinesq's approximation.
ii. It is assumed that the magnetic Reynolds number is very small, which corresponds to a negligibly induced magnetic field compared to the externally applied one.
iii. The plates are assumed to be heated asymmetrically, with one plate maintained at a temperature T_0 while the other plate is at a temperature T_h.
iv. Due to this temperature gradient between the plates, it is assumed that natural convection flow occurs in the microchannel.
v. The effect of Soret is taken into consideration
vi. The fluid is assumed to be saturated with Darcy porous material

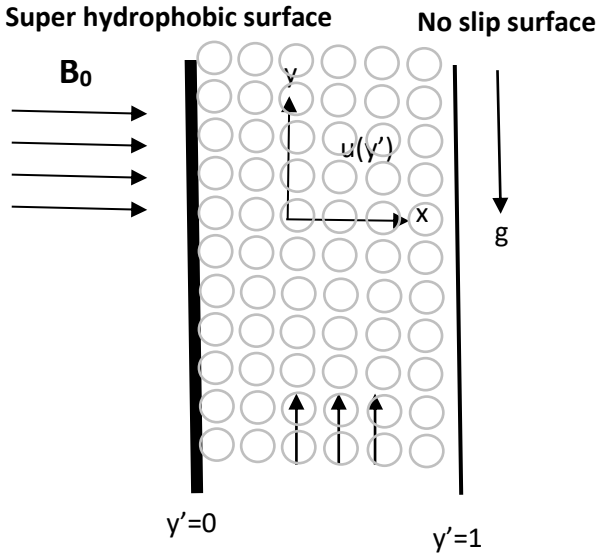

Figure 1: Sketch of the flow System

Following Omokhuale and Ojemeri (2025) and Hamza *et al*. (2024c), the present problem in dimensional form can be written as:

$$V\frac{d^2u'}{dy'^2} + g\beta_0(T' - T_O) + g\beta_1(\emptyset' - \emptyset_O) - \frac{\sigma B_O^2 u'}{\rho} - \frac{u'}{K} = 0 \quad (1)$$

$$\frac{k}{\rho c_\rho}\frac{d^2T'}{dy'^2} + \frac{QC_0^* A}{\rho c_\rho} e^{\left(\frac{-E}{RT'}\right)} = 0 \quad (2)$$

$$D\frac{d^2\emptyset'}{dy'^2} + \frac{DK_T}{T_m}\frac{d^2T'}{dy'^2} = 0 \quad (3)$$

With boundary conditions:

DOI: https://doi.org/10.57233/ihcfs.026

ISBN: 978-978-68-07775

BOOK OF PROCEEDINGS

IHCFS – 2025 WEBSITE: fos.fugusau.edu.ng

$$\left.\begin{array}{l}\left.\begin{array}{l} u(y') = \gamma' \frac{du'}{dy'} \\ T(y') = T_h + \Gamma' \frac{dT'}{dy'} \end{array}\right\} at\ y' = 0 \\ \emptyset' = \emptyset_w \\ \left.\begin{array}{l} u(y') = 0 \\ T(y') = T_o \end{array}\right\} \qquad at\ y' = L \\ \emptyset' = -\emptyset_w \end{array}\right\} \tag{4}$$

Introducing the dimensionless quantities as:

$$u = \frac{u'}{U}, y = \frac{y'}{h}, \theta = \frac{T' - T_0}{T_w - T_o}, x = \frac{x'v}{Uh^2}, M^2 = \frac{\sigma\beta_o^2 h^2}{\rho v}, (Y, \gamma, \Gamma) = (Y', \gamma', \Gamma')/h$$

$$\emptyset = \frac{C' - C_0}{C_w - C_o}, \mathrm{N} = \frac{g\beta^*(T_w - T_o)H^2}{vU}, \mathrm{S}_o = \frac{\mathrm{D}_m \mathrm{K}_T (T_\prime - T_o)}{vT_\prime (C_\prime - C_o)}, \varepsilon = \frac{RT_0}{E}, \lambda = \frac{QC_0^* AEH^2}{RT_0^2}, Da = \frac{k}{L^2}, \tag{5}$$

inserting eqn (5) into eqns (1-4), the governing equations of the velocity and temperature become:

$$\frac{d^2U}{dy^2} + \theta + \mathrm{N}\emptyset - M_1^2 U = 0 \tag{6}$$

$$\frac{d^2\theta}{dy^2} + \lambda e^{\frac{\theta}{1+\varepsilon\theta}} = 0 \tag{7}$$

$$\frac{d^2\emptyset}{dy^2} + S_o \left[\frac{d^2\theta}{dy^2}\right] = 0 \tag{8}$$

The boundary conditions are:

$$\begin{array}{llll} \emptyset(y) = R_c, & \theta(y) = 1 + \Gamma \frac{d\theta}{dy}, & u(y) = \gamma \frac{du}{dy} & \text{at } y = 0 \\ \emptyset(y) = -R_c, & \theta(y) = 0, & u(y) = 0 & \text{at } y = 1 \end{array} \tag{9}$$

Where $M_1^2 = M^2 + \frac{1}{Da}$, M is the magnetic parameter, N is the sustention parameter, λ is the viscous heating parameter, ε is the activation energy, S_o is the thermal diffusion parameter, R_c is the wall concentration parameter, Γ is the temperature jump parameter, and γ is the velocity slip parameter.

Closed Form Solution

The regular perturbation technique is used to address the coupled nonlinear guiding equations. The velocity, temperature, and mass diffusion solutions are considered to be as follows:

$$U = u_0 + \lambda(u_1) \tag{10}$$

$$\theta = \theta_0 + \lambda(\theta_1) \tag{11}$$

$$\emptyset = \emptyset_0 + \lambda(\emptyset_1) \tag{12}$$

By introducing equations (8) and (9) into equations (5) to (7) and obtaining the coefficients of λ^0 and λ, we obtain a new system of ordinary differential equations with their associated boundary conditions as:

$$\lambda^0: \frac{d^2u_0}{dy^2} - M_1^2 u_0 = -\theta_0 - \mathrm{N}\emptyset_0 \tag{13}$$

$$\lambda: \frac{d^2u_1}{dy^2} - M_1^2 u_1 = -\theta_1 - \mathrm{N}\emptyset_1 \tag{14}$$

DOI: https://doi.org/10.57233/ihcfs.026

ISBN: 978-978-68-07775

BOOK OF PROCEEDINGS

IHCFS – 2025 WEBSITE: fos.fugusau.edu.ng

$$\lambda^0: \frac{d^2\theta_0}{dy^2} = 0 \quad (15)$$

$$\lambda: \frac{d^2\theta_1}{dy^2} + 1 + \theta_0 + (\frac{1}{2} - \varepsilon)\theta_0^2 = 0 \quad (16)$$

$$\lambda^0: \frac{d^2\emptyset_0}{dy^2} + S_o \frac{d^2\theta_0}{dy^2} = 0 \quad (17)$$

$$\lambda: \frac{d^2\emptyset_1}{dy^2} + S_o \frac{d^2\theta_1}{dy^2} = 0 \quad (18)$$

$$\left.\begin{array}{l} \lambda^0: \theta_o = 1 + \Gamma\frac{d\theta_o}{dz} \\ \lambda: \theta_1 = \Gamma\frac{d\theta_1}{dz} \\ \lambda^0: u_0 = \gamma\frac{dU_o}{dz} \\ \lambda: u_1 = \gamma\frac{dU_1}{dz} \\ \lambda^0: \emptyset_0 = R_c \\ \lambda: \emptyset_1 = 0 \end{array}\right\} \text{at } y = 0 \quad (19)$$

and

$$\left.\begin{array}{l} \lambda^0: \theta_0 = 0 \\ \lambda: \theta_1 = 0 \\ \lambda^0: u_0 = 0 \\ \lambda: u_1 = 0 \\ \lambda^0: \emptyset_0 = -R_c \\ \lambda: \emptyset_1 = 0 \end{array}\right\} \text{at } y = 1 \quad (20)$$

The solutions of velocity, temperature and concentration are derived as:

$$u_0 = F_1\cosh(M_1 y) + F_2 sinh(M_1 y) + F_3 y + F_4 \quad (21)$$

$$u_1 = F_5\cosh(M_1 y) + F_6 sinh(M_1 y) + F_7 y^4 + F_8 y^3 + F_9 y^2 + F_{10} y + F_{11} \quad (22)$$

$$\theta_0 = J_1 y + J_2 \quad (23)$$

$$\theta_1 = -\frac{y^2}{2} - J_1\frac{y^6}{3} - J_2\frac{y^2}{2} - a_1(J_1^2\frac{y^4}{12} + J_1 J_2\frac{y^3}{3} + J_2^2\frac{y^2}{2} + J_3 y + J_4) \quad (24)$$

$$\emptyset_0 = D_1 y + D_2 \quad (25)$$

$$\emptyset_1 = S_0\frac{y^2}{2} + S_0 J_1\frac{y^3}{6} + S_0 J_2\frac{y^2}{2} + S_0 a_1\left(J_1^2\frac{y^4}{12} + J_1 J_2\frac{y^3}{3} + J_2^2\frac{y^2}{2} + J_3 y + J_4\right) + D_3 y + D_4 \quad (26)$$

Where the skin friction, Nusselt number and rate of mass transfer are calculated as:

$$\frac{dU}{dy}\Big|_{y=0} = M_1 F_2 + F_3 + \lambda[M_1 F_6 + F_{10}] \quad (27)$$

$$\frac{dU}{dy}\Big|_{y=1} = M_1 F_1\sinh(M_1) + M_1 F_2\cosh(M_1) + F_3 + \lambda[M_1 F_5\sinh(M_1) + M_1 F_2\cosh(M_1) + 4F_7 + 3F_8 + 2F_2 + F_{10}] \quad (28)$$

$$\frac{d\theta}{dy}\Big|_{y=0} = J_1 + \lambda J_3 \quad (29)$$

$$\frac{d\theta}{dy}\Big|_{y=1} = J_1 + \lambda\left[-2J_1 - 2J_2 - a_1\left(\frac{J_1^2}{3} + J_1 J_2 + J_2^2 + J_3\right)\right] \quad (30)$$

$$\frac{d\emptyset}{dy}\Big|_{y=0} = D_1 + \lambda(D_3) \quad (31)$$

$$\frac{d\emptyset}{dy}\Big|_{y=1} = D_1 + \lambda\left[S_0 + S_0\frac{J_1}{2} + S_0 J_2 + S_0 a_1(\frac{J_2^2}{3} + J_1 J_3 + J_2)D_3\right] \quad (32)$$

DOI: https://doi.org/10.57233/ihcfs.026

ISBN: 978-978-68-07775

BOOK OF PROCEEDINGS

IHCFS – 2025 WEBSITE: fos.fugusau.edu.ng

DISCUSSION OF THE FINDINGS

Analytically, the thermal diffusion impact on Arrhenius-governed heat transfer flow with uniform wall concentration influence along a microchannel occupied with SHS is investigated. The resulting stable ordinary differential equations are treated using a semi-analytical technique. Several graphs have been created to showcase the effects of various factors. The reference values selected for this analysis are (γ = Γ= 1, N =5, R_c=0.1, M=0.5, Da=0.1, $S_0 = 1\ and\ \lambda$ = 0.001).

To determine the precision and correctness of the current study, Figure 2 depicts a numerical comparison between the work of Omokhuale and Ojemeri (2025) and the current work. The graphical comparison indicates a good agreement.

The variation of the Darcy porous medium, Da, on the velocity gradient is plotted in Figure 3. It is seen that raising the values yields better flow movement in the microchannel. This is understandably true mainly due to the viscosity drag of the fluids' inertia. The fluid acts as the carrier medium and, as it moves, it exerts a drag force on the fluid, accelerating it. Figure 4 illustrates the influence of R_c on the mass diffusion variation. The illustration shows that a greater level of R_c increases the concentration of the fluid near the left wall while decreasing it near the right wall. This is due to the symmetrical character of the wall concentration parameter. However, there is a point of intersection in the middle of the microchannel where the flow is unaffected by the parameter being considered. This conclusion is extremely valuable in the creation and control of reverse flow. Furthermore, the results from this investigation are consistent with those reported by Hamza et al. (2024c). Figure 5 explains how R_c affects the velocity profile. It is found that the influence of temperature on fluid flow causes the reversal to start faster at the top plate before increasing considerably towards the bottom plate. Figure 6 shows the influence of S_0 on the mass diffusion gradient. A rise in the Soret effect suggests increased molar mass diffusivity. Molecular mass diffusivity causes a rise in concentration. This demonstrates that the species concentration in the fluid increases as the Soret number increases. Figure 7 shows how the Soret number affects fluid velocity. It is apparent that when the Soret number increases, fluid mobility improves. This implies that the fluid velocity is accelerated by the Soret number across the boundary layer area. A surge in the number of Sorets indicates a reduction in the viscosity of the fluid. Consequently, the implications of viscosity and drag are amplified. Hence, the velocity of the fluid increases. Figures 8 and 9 show the variations of λ on the temperature and velocity distributions. Increasing the value of λ leads to a drastic growth in the temperature and velocity gradients. This is attributed to the fact that a rise in temperature causes a drop in the fluid viscosity and an increase in fluid velocity as λ increases. As a result, the gas flows quickly toward the wall. Additionally, the fluid wall effect decreases when velocity slip increases at the SHO walls. Figures 10a and b show the effect of R_c versus γ on the shearing stress. It is revealed that rising values of R_c heighten the skin friction at both microchannel plates due to the nature of symmetric wall conditions. Figures 11a and b demonstrate how S_0 and γ affect skin friction on both upstanding walls. Figure 11a shows that near the wall (y=0), the shearing stress is significantly strengthened; however, when y=1, the reverse case happens as plotted in Figure 11b. The function of Da on the skin friction coefficient is displayed in Figures12a and b. These figures depict that the increasing Darcy porous parameter strengthens the skin friction at both plates. Figures 13a and b display how altering S_0 affects the Sherwood number. It is observed that raising the value of S_0 brings down the rate of mass transfer. It was noticeable that elevating R_c strengthens

DOI: https://doi.org/10.57233/ihcfs.026

ISBN: 978-978-68-07775

the skin friction at both microchannel plates due to the nature of uniform wall heating conditions.

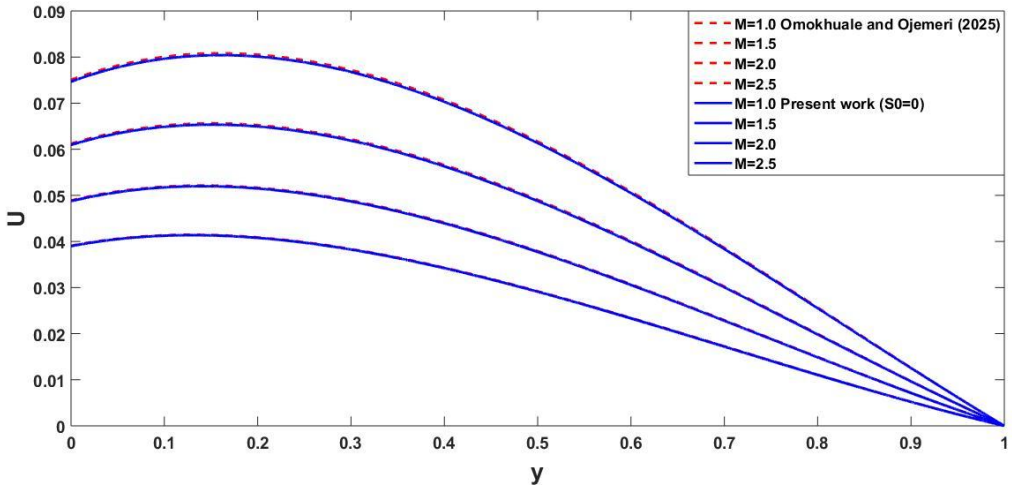

Figure 2: Graphical comparison between the present work and that of Omokhuale and Ojemeri (2025)

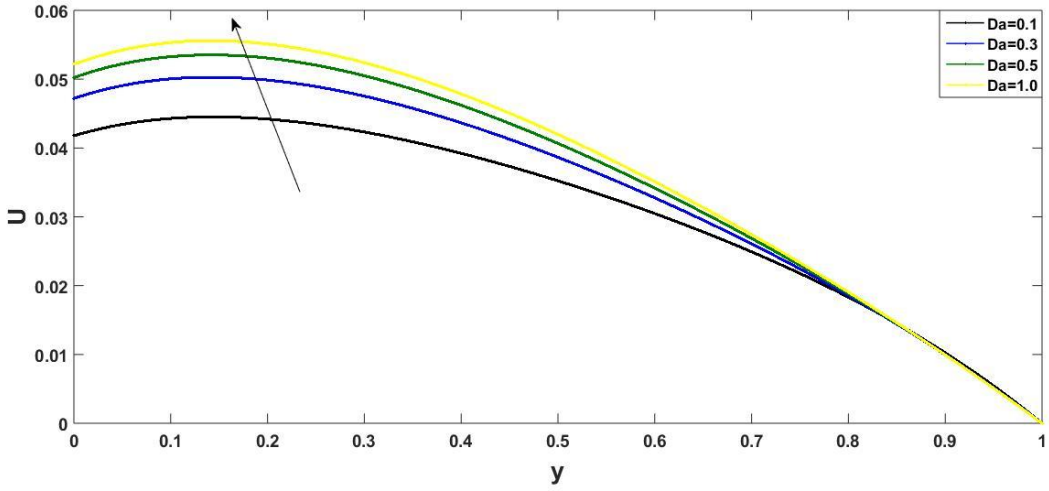

Figure 3: Result of Da on the Velocity profile

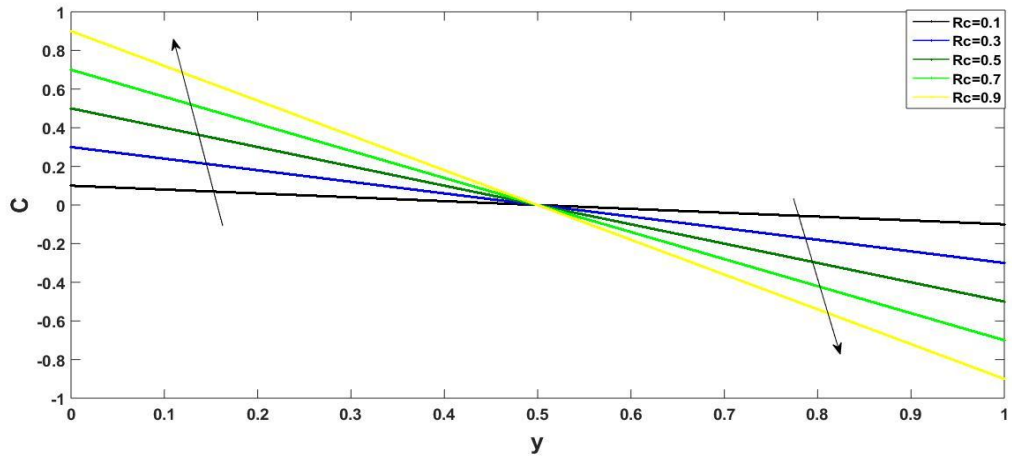

DOI: https://doi.org/10.57233/ihcfs.026

ISBN: 978-978-68-07775

BOOK OF PROCEEDINGS

Figure 4: Result of R_c on the Concentration profile

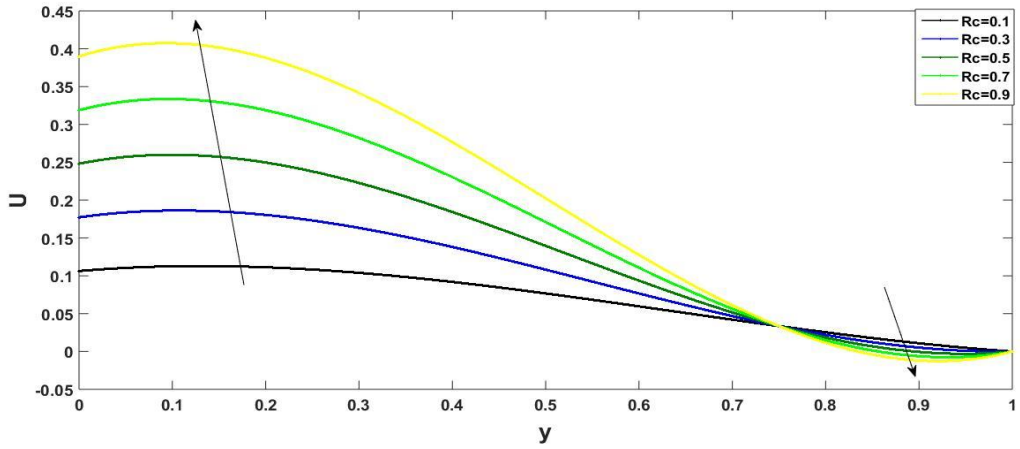

Figure 5: Result of R_c on the Velocity profile

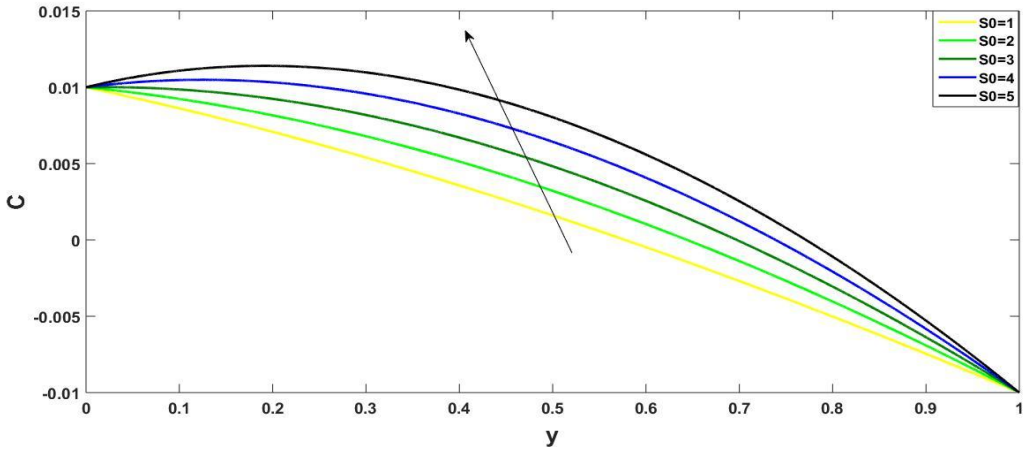

Figure 6: Result of S_0 on the Concentration profile

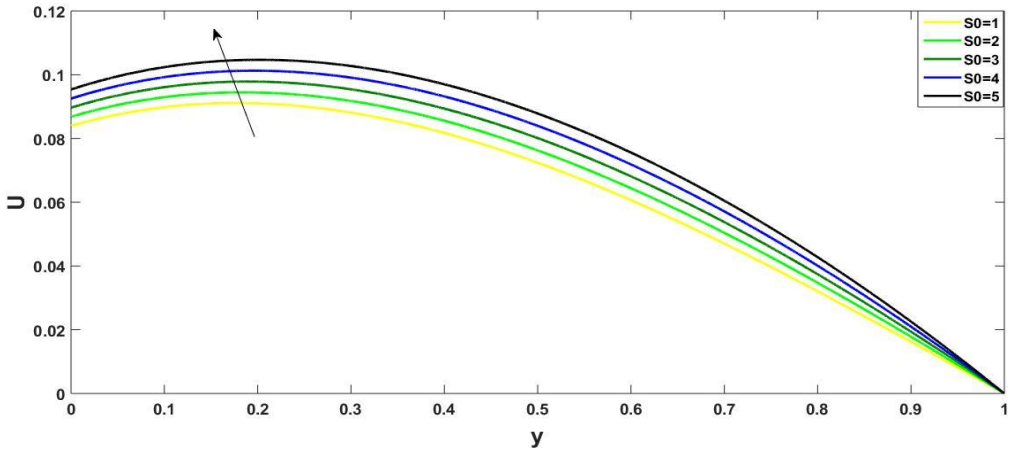

Figure 7: Result of S_0 on the Velocity profile

DOI: https://doi.org/10.57233/ihcfs.026

ISBN: 978-978-68-07775

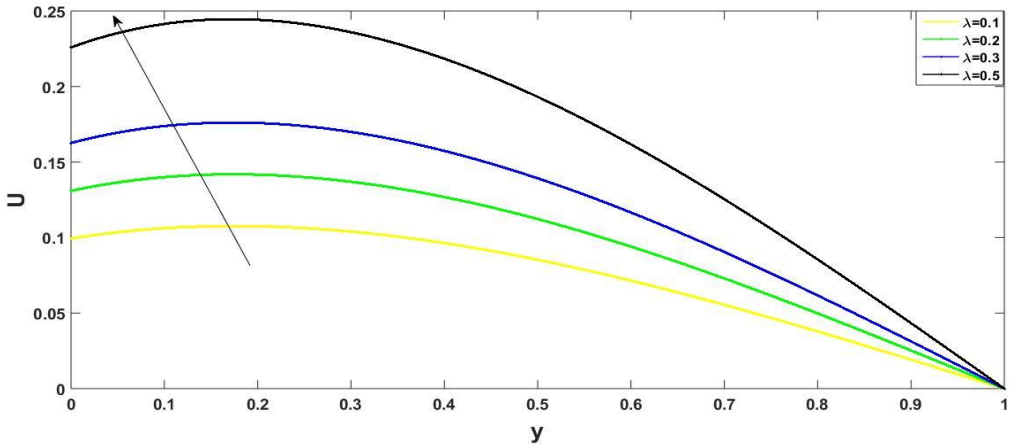

Figure 8: Result of λ on the Velocity profile

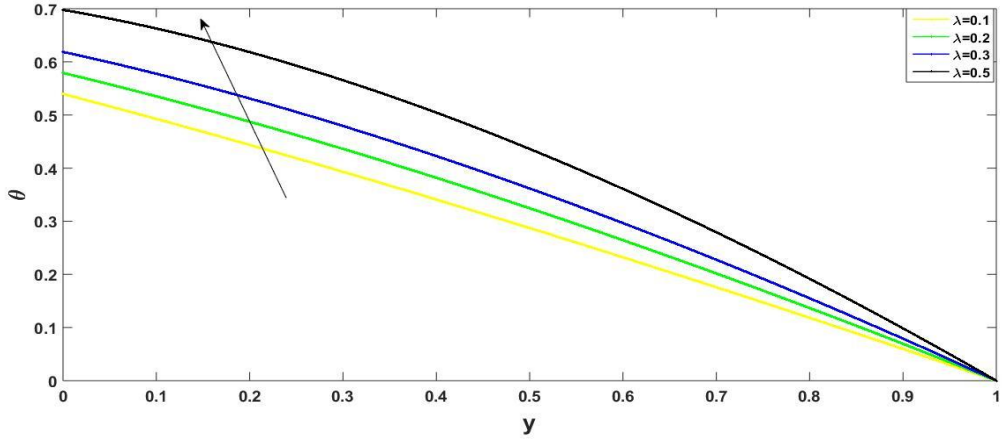

Figure 9: Result of λ on the Temperature profile

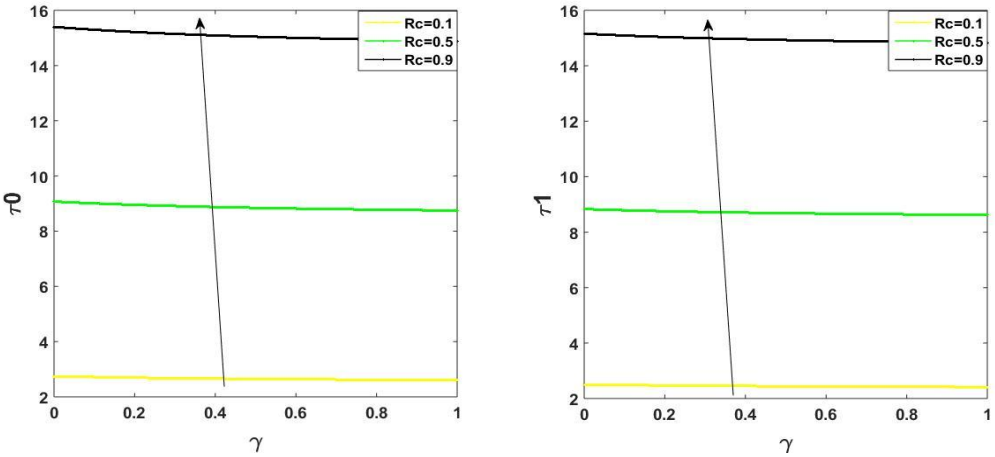

Figure 10: Result of R_c on the Skin Friction

DOI: https://doi.org/10.57233/ihcfs.026

ISBN: 978-978-68-07775

BOOK OF PROCEEDINGS

IHCFS – 2025 WEBSITE: fos.fugusau.edu.ng

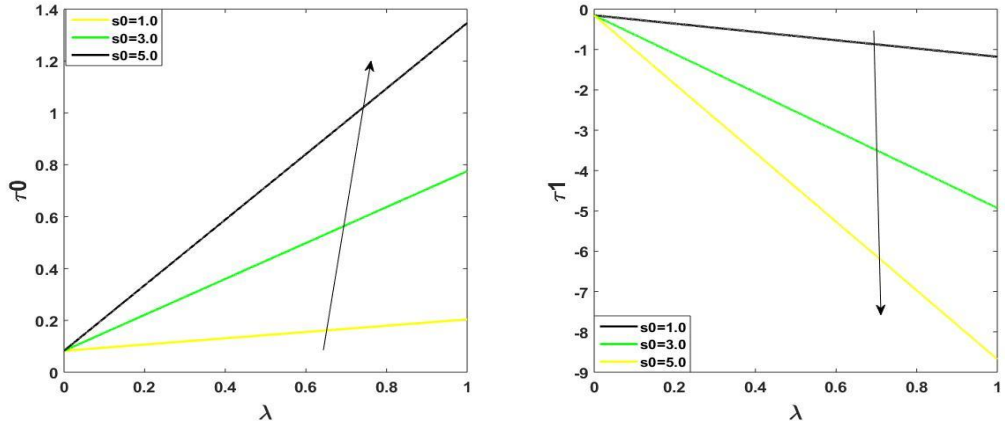

Figure 11: Result of S_0 on the Skin Friction

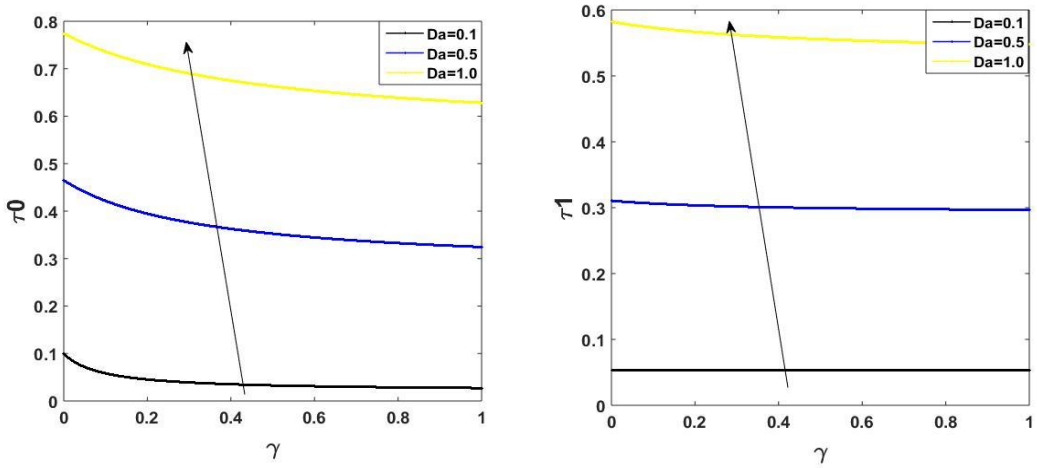

Figure 12: Result of Da on the Skin Friction

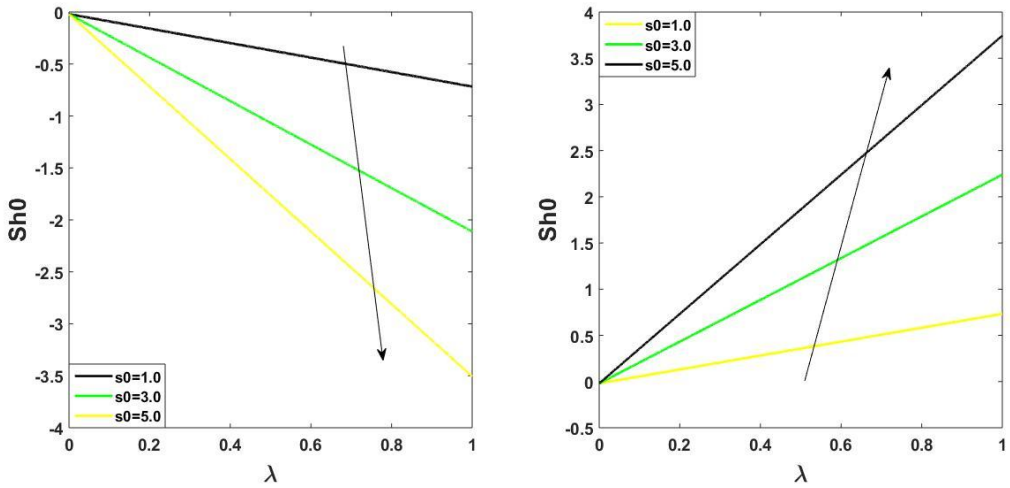

Figure 13: Result of S_0 on the Sherwood number

DOI: https://doi.org/10.57233/ihcfs.026

ISBN: 978-978-68-07775

BOOK OF PROCEEDINGS

Validation of Results

Setting S_0 to be zero, and Da=1000, the work of Omokhuale and Ojemeri (2025) is successfully retrieved, establishing a good concurrence between the present study and their work as demonstrated in Figure 2.

CONCLUSION

This study looked at the effects of thermo-diffusion and symmetric wall concentration on heat and mass transfer flow in a magnetized exothermic fluid over a porous microchannel with SHO features. A semi-analytical (regular perturbation) technique is employed to treat the unique ordinary differential equations that govern the flow in terms of concentration, temperature, and velocity components. The effect of major fluid parameters is depicted via line graphs. These results are compared to earlier work for the limiting situation $(S_0 = 0 \; and \; Da = 1000)$, and they agree quite well. This model will inform environmental studies, such as the prediction of contaminant transport in the subsurface and the design of remediation systems, facilitating environmental protection and risk assessments. Some intriguing findings from this article are summarized below:

(i) The action of Darcy porous medium is anticipated to promote the hydromagnetic flow in the microchannel.

(ii)The velocity and concentration of the fluid are strongly influenced by the action of the symmetric wall concentration. Flow reversal is observed as the symmetric wall concentration increases.

(iii) The presence of the Soret effect is seen to amplify the fluid flow and mass diffusion in the microchannel

(iv) The effect of λ is envisaged to improve the velocity and temperature gradients, respectively.

(v) It was concluded that higher values of R_c parameter favor the skin friction at both plates of the microchannel.

(vi) It is concluded that increasing the Darcy porous parameter strengthens skin friction at both plates.

(vii) The shearing stress is stronger at the surface (y = 0) for growing level of M and S_0 respectively, whereas a counter attribute happens at (y = 1).

(viii) The rate of mass transfer demonstrates a reducing trend in the presence of S_0 at the plate (y = 0), whereas a reverse phenomenon is seen at y=1.

(ix) In the future, the effect of mixed convection will be considered on this model.

REFERENCES

Ahmed N., Deka H., Haloi P. (2024). MHD Mass Transfer Flow in Presence of Chemical Reaction, Thermal Radiation, and Thermal Diffusion Effect, Heat Transfer, Wiley, 54(2), 1358-1375.

Akhtari, M. R. and Karimi, N. (2020). Thermohydraulic analysis of a microchannel with varying superhydrophobic roughness. Applied Thermal Engineering, 172, https://doi.org/10.1016/j.applthermaleng.2020.115147

Babu B. H., Swarnalathamma B. V., Krishna M. V. (2024). Diffusion-thermo and thermo-diffusion impacts on MHD natural convection flow of Maxwell nanofluids over a stretching sheet, *Case Studies in Thermal Engineering,* 61, 105016.

Bafakeeh O. T., Raza A., Khan U. S., Khan M. I., Nasr A., Khedher N.B. and Tag-Eldin E.M. (2022). Physical interpretation of Nanofluid (Copper Oxide and Silver) with slip and mixed convection effects: Application of fractional derivatives; *Applied Sciences*, 12 (21), 10860.

Baoku, I. and Fadare, S.A. (2018). Thermo-diffusion and diffusion -thermo effects on mixed convection hydromagnetic flow in a third-grade fluid over a stretching surface in a Darcy forchheimer porous medium. *FUDMA Journal of Sciences*, 2(1), pp. 23-42.

Bordoloi R., Chamuah K. and Ahmed N. (2023). Free Convective MHD Radiative Flow Past a Porous Vertical Plate in a Porous Medium with Chemical Reaction, Biointerface Research in Applied Chemistry, 13 (3), pp. 1-15.

Chamuah K., and Ahmed N. (2021). MHD free convective dissipative flow past a porous plate in a porous medium in the presence of radiation and thermal diffusion effects. Heat Transfer, 51, 1964-1981, https://doi.org/10.1002/htj.22383.

Hamza M. M., Ahmad S. K., Ojemeri G., Usman H. and Shuaibu A. (2023b). Exploring the dynamics of an exothermic chemical reaction controlled by Arrhenius kinetics with Hall effect in a microchannel, *FUDMA Journal of Sciences,* 7(3), 112-124.

Hamza, M. M., Balarabe A. Y., Ibrahim M., Akpootu D. O. and Sheriff A. (2025). Transient fractional dusty fluid flow in a superhydrophobic microchannel, *European Physical Journal Plus,*140, 366, pp 1-17.

Hamza, M. M., Bello S. R., Ibrahim Y., Bello A. and Tasiu R. A. (2024c). Casson fluid flow with heat sink affected by symmetric wall temperature and concentration conditions, *Journal of Engineering Technology,* 15(2). https://doi.org/10.54554/jet.2024.15.2.002

Hamza, M. M., Shehu, A., Muhammad, I., Shuaibu, A., Ojemeri, G. (2024a). Electro-kinetically free convective heat flow in a slit microchannel, *International Journal of Applied and Computational Mathematics,* 10, https://doi.org/10.1007/s40819-024-01765-x

Hamza, M. M., Shehu, A., Muhammad, I., Shuaibu, A., Ojemeri, G. (2024b). Electrokinetically controlled mixed convective heat flow in a slit microchannel, *Heat Transfer,* DOI:10.1002/htj.23104

Hamza, M. M., Shuaibu, A., Ahmad, S. K. (2022). Unsteady MHD free convection flow of an exothermic fluid in a convectively heated vertical channel filled with porous medium, *Scientific Reports*, **12**, 11989.

Heidarian, A., Rafee, R., Valipour, M. S. (2020). Effects of wall hydrophobicity on the thermohydraulic performance of the microchan nels with nanofluids. Int. Comm. Heat and Mass Transfer, 117, https://doi.org/10.1016/j.icheatmasstransfer.2020.104758

Jha, B. K. and Gwandu, B. J. (2018). MHD free convection flow in a vertical slit micro-channel with super- hydrophobic slip and temperature jump: Heating by constant wall temperature. Alexandria Engineering Journal, 57, https://dx.doi.org/10.1016/j.aej.2017.08.022

Jha, B. K. and Gwandu, B. J. (2020). MHD free convection flow in a vertical porous super-hydrophobic microchannel. J. Proc. Mech. Eng., 235 (2).

Kattimani P., Patil N., Kalia R., Sahana B., Sunitha M., Nagaraja K. V. (2024). Analysis of thermal diffusion and diffusion thermo effects under the condition of pollutant concentration and bio-convection: An artificial neural network approach, *International Journal of Thermofluids,* 27, 101235

Lee H., Fridlind A. M. and Ackerman A. S. (2021). An evaluation of size-resolved cloud microphysics scheme numerics for use with radar observations, Part II: condensation and evaporation, J. Atmos. Sci., 78(5), 1629-1645. DOI:10.1175/JAS-D-20-0213.1.

Ojemeri, G. and Onwubuya, I. O. (2023a). Exploring the dynamics of viscous dissipative fluid past a super-hydrophobic microchannel in the coexistence of mixed convection and porous medium, *Saudi Journal of Engineering Technology*, **8**, pp.71-80.

Ojemeri, G. and Onwubuya, I. O. (2023b). Analysis of mixed convection flow on Arrhenius-controlled heat generating/absorbing fluid in a superhydrophobic microchannel: A semi-analytical approach, *Dutse Journal of Pure and Applied Sciences,* 9a**,** 344-357.

Ojemeri G. and Onwubuya I. O. (2023c). Investigation of Arrhenius-controlled chemical reaction through a superhydrophobic microchannel, *FUDMA Journal of Sciences,* 7(3), 80-86.

Ojemeri G. and Onwubuya I. O. (2023d). Significance of viscous dissipation and porosity effects in a heated superhydrophobic microchannel, *Journal of Engineering and Technology (JET),* 14(2), 1-19.

Ojemeri G., Hamza M. M., Agnes Marian Ochiba A. M., Onwubuya I. O., Adeniran Kolade Ademuwagun A. K., Muhammad A. T., Ahmad I. S. (2025). Thermal radiation effect on a bouyancy-induced couette flow due to Newtonian heating in an upstanding channel, *Fulafia Journal of Science and Technology*, 9(2). 9-18. https://doi.org/10.62050/fjst2025.v9n2.498

Ojemeri G., Hamza M. M., Haliru B. T., Bello I. and Shuaibu A. (2023). Influence of Soret and Radial Magnetic Field on Natural Convection of a Chemically Reactive Fluid in an Upright Porous Annulus, UMYU Scientifica, 2(3), 108-120.

Ojemeri, G. and Hamza, M. M. (2022). Heat transfer analysis of Arrhenius-controlled free convective hydromagnetic flow with heat generation/absorption effect in a micro-channel, *Alexandria Eng. J.*, **61**, pp. 12797-12811.

Ojemeri, G., Onwubuya I. O., Omokhuale, E., Hussaini A. and Shuaibu, A. (2024). Analytical investigation of Arrhenius kinetics with heat source/sink impacts along a heated superhydrophobic microchannel, UMYU

Scientifica, 3(1), 61-71. DOI:105619/usci.2431.004.

Ojemeri, G., Onwubuya I. O., Shuaibu A., Omokhuale, E. and. Altine M. M. (2023c). Arrhenius-controlled heat transfer fluid provoked by porosity effect through a vertical microchannel: An analytical approach, *Continental Journal of Applied Sciences,* 18(1), 18-40.

Omokhuale E. and Dange M. S. (2023). Natural convection Couette flow in the presence of magnetic field and thermal property. International Journal of Science for Global Sustainability, 9(2), 10 – 20. Doi.org/10.57233/ijsgs.v9i2.453.

Omokhuale E. and Ojemeri G. (2025). Arrhenius-controlled fluid flow over a superhydrophobic microchannel with symmetric wall concentration, *Journal of Basic Physical Research,* 14(1) pp. 77 – 90. https://journals.unizik.edu.ng/jbpr/

Omokhuale E., Abubakar J. and Ojemeri G. (2024b). Mixed Convection Flow of a Magnetized Nanofluid with Viscous Dissipation in an Oscillatory System, *International Journal of Science for Global Sustainability,* 10(2), pp. 229-241. DOI: https://doi.org/10.57233/ijsgs.v10i2.672.

Omokhuale E., Ojemeri G., Muhammad A. and Usman H. (2024a). Significance of Viscous Dissipation on Hydromagnetic Oscillatory Flow Affected by Nanoparticles Through a Boundary Layer Regime, International Journal of Development Mathematics 1(1), pp. 098-113.

Prakash D. and Sivakumar N. (2018). Influence of viscous and ohmic heating on mhd flow of nanofluid over an inclined nonlinear stretching sheet embedded in a porous medium, *International Journal of Mechanical Engineering and Technology (IJM ET),* 9(8), pp. 992-1001.

Sharma, H., Gaddam, A., Agrawal, A., Joshi, S.S. and Dimov, S. S. (2020). Influence of texture shape and arrangement on thermo-hydraulic performance of textured microchannels. Int. J. Therm. Sci., 147, https://doi.org/10.1016/j.ijthermalsci.2019.106146

Sia, G. D., Lim, C.S., Tan, M.K., Chen, G.M. and Hung, Y. M. (2023). Anomalously enhanced subcooled flow boiling in superhydrophobic graphene-nanoplatelets'-coated microchannels. Int. Comm. Heat and Mass Transfer, 146, https://doi.org/10.1016/j.icheatmasstransfer.2023.106932

Sravanthi, C. S., Gorla, R. S. R. (2018). Effects of heat source/sink and chemical reaction on MHD Maxwell nanofluid flow over a convectively heated exponentially stretching sheet using Homotopy analysis method, *Int. J. Appl. Mech. Eng.* 23(1), pp. 137–159.

Uka U. A., Emeziem I. C., Ayinde S. A., Adenika C. and K. O. Agbo (2023). Enhancement of heat transfer with viscous dissipation impact on fluid flow past a moving wedge in a permeable domain, *Eskişehir Technical University Journal of Science and Technology A- Applied Sciences and Engineering,* 24(3), pp. 164-176, DOI:10.18038/estubtda.1197024

Usman and Sanusi (2023). Heat and mass transfer analysis for the MHD flow of Casson nanofluid in the presence of thermal radiation, *FUDMA Journal of Sciences,* 7(2), pp 188 – 198.

Yale I. D., Uchiri A. M. T., Hamza M. M., and Ojemeri G. (2023). Effect of viscous dissipation fluid in a slit microchannel with heated superhydrophobic surface, *Dutse Journal of Pure and Applied Sciences,* 9(3b), pp. 290-302.

Zhang, W., Wang, Q., Zeng, M., and Zhao, C. (2019). Thermoelectric effect and temperature-gradient-driven electrokinetic flow of electrolyte solutions in charged nanocapillaries. *International Journal of Heat and Mass Transfer, 143, https://*doi:10.1016/j.ijheatmasstransfer.2019.118569.

Appendix

$$D_2 = R_c, D_1 = -2R_c, D_3 = -\frac{S_0}{2} - \frac{S_0 J_1}{6} - \frac{S_0 J_2}{2} - S_0 J_2\left(\frac{J_1^2}{12} + \frac{J_1 J_2}{3} + J_3 + J_4\right), D_4 = 0, J_1 = -J_2, J_2$$

$$= \frac{1}{1+\Gamma}, J_3 = \frac{\left(\frac{1}{2} + \frac{J_1}{6} + \frac{J_2}{2} + a_1\frac{J_1^2}{12} + a_1\frac{J_1 J_2}{3} + a_1\frac{J_2^2}{2}\right)}{1+\Gamma},$$

$$J_4 = \Gamma J_3, F_1 = \gamma[M_1 F_3 + F_4] - F_5, F_2 = \frac{-\gamma F_3 cosh(M_1) + F_4 cosh(M_1)}{\gamma M cosh(M_1) + sinh(M_1)},$$

$$F_3 = \frac{J_1}{M_1^2}, F_4 = \frac{J_2 + 2F_2}{M_1^2}, F_5 = \gamma[M_1 F_6 + F_{11}] - F_{12},$$

$$F_6 = \frac{-S_0(a_{10} + a_9)}{\gamma M_1 cosh(M_1) + sinh(M_1)}, F_7 = \frac{-S_0 a_3}{M_1^2}, F_8 = \frac{-S_0 a_4}{M_1^2}, F_9 = \frac{S_0(a_3 + 20F_9)}{M_1^2},$$

DOI: https://doi.org/10.57233/ihcfs.026

ISBN: 978-978-68-07775

$$F_{10} = \frac{S_0(a_6 + 12F_8)}{M_1^2}, F_{11} = \frac{S_0(a_7 + 6J_{14})}{M_1^2}, J_{17} = \frac{S_0(a_8 + 2J_{15})}{M_1^2}, a_1 = \frac{1}{2} - \varepsilon,$$

$$a_2 = J_7 + J_8 + J_{9,}\ a_4 = \frac{J_1^2 a_1}{12}, a_5 = \frac{J_1}{6} + \frac{J_1 J_2 a_1}{3}$$

$$a_8 = -J_4\ a_9 = F_9 + F_8 + F_9 + F_{10} + F_{11} + F_{12}, a_{10} = (\gamma F_{11} - F_{12})cosh(M_1)$$